A NUMERICAL STUDY ON CHARACTERISTICS OF FLUID FLOW AND SOLUTE TRANSPORT IN A SELF-AFFINE VARIABLE-APERTURE FRACTURE UNDER NORMAL COMPLIANCE EFFECT

WOOCHANG JEONG[1], MANHA HWANG[2], ICKHWAN KO[3], JAIWOO SONG[4]

[1] Senior Researcher, Hydrosystems Engineering Center, Korea Institute of Water and Environment, Korea Water Resources Corporation, 462-1 Jeonmin-Dong, Yusung-Gu, Daejeon, 305-730, Korea
(Tel: 82-42-860-0433, Fax: 82-42-860-0349, e-mail: jeongwc@kowaco.or.kr)

[2] Head Researcher, Hydrosystems Engineering Center, Korea Institute of Water and Environment, Korea Water Resources Corporation, 462-1 Jeonmin-Dong, Yusung-Gu, Daejeon, 305-730, Korea
(Tel: 82-42-860-0345, Fax: 82-42-860-0349, e-mail: mhhwang@kowaco.or.kr)

[3] Director, Hydrosystems Engineering Center, Korea Institute of Water and Environment, Korea Water Resources Corporation, 462-1 Jeonmin-Dong, Yusung-Gu, Daejeon, 305-730, Korea
(Tel: 82-42-860-0345, Fax: 82-42-860-0349, e-mail: ihko@kowaco.or.kr)

[4] Professor, Department of Civil Engineering, Hongik University, 72-1, Sangsu-Dong, Mapo-Gu, Seoul, 121-791, Korea
(Tel: 82-2-320-1650, Fax: 82-2-325-2332, e-mail: jwsong@hongik.ac.kr)

Abstract: This paper presents the numerical study to examine characteristics of fluid flow and solute transport in a rough fracture subject to effective normal stresses. The aperture distribution is generated by using the self-affine fractal model. In order to represent a nonlinear relationship between the supported normal stress and the fracture aperture, we combine a simple mechanical model with the local flow model. The solute transport is simulated using the random walk particle following algorithm. Results of numerical simulations show that the flow is significantly affected by the geometry of aperture distribution varying with the effective normal stress level while it is slightly affected by the fractal dimension that determines the degree of the fracture surface roughness. However, solute transport is influenced by the effective normal stress as well as the fracture surface roughness.

Keywords: Single fracture, nonlinear Hydromechanical effect, Fracture network, Self-affine fractal model, Fractal dimension

1. INTRODUCTION

Faults and fractures play an important role in the transport of fluid and solute through rocks with low permeability. Under a wide range of circumstances these transport processes are concentrated onto a network of interconnected individual fractures and thus it is important to

analyze the fluid flow and solute transport in a single fracture. The flow and transport behaviors in a fracture depend significantly on the distribution of void spaces between two opposing fracture walls and also on the roughness of the fracture surface (Gentier, 1986). It is well recognized that the fractures include closed regions where two walls are in contact each other, as well as opened regions where two walls are separated by a distance that is varied from point to point. The aperture and contact area distributions in the fracture depend significantly on the normal (e.g. Durham and Bonner, 1995) or shear stress (e.g. Yeo et al., 1998) acting on the fracture. In general, the effect of both stresses tends to decrease the void spaces offered to the fluid flow and solute transport due to the increase of contact areas.

In the present work, the flow and transport behaviors in a variable-aperture fracture subjected to only normal stresses are numerically analyzed. The variable aperture distribution in the fracture is generated by using the self-affine fractal model and the fracture surface roughness is represented by the fractal dimension. In order to represent a nonlinear relationship between the effective normal stress and the fracture aperture, a simple mechanical model is adapted and combined with the local flow model. The effect of the fractal dimension on the flow and transport behaviors is also examined.

2. GENERATION OF FRACTAL APETURE FIELD

The fluid flow in a natural single fracture is sensible to the distribution of variable apertures (Gentier, 1986). Most of detailed measures for the aperture distribution were performed by laboratory experiments with natural fracture samples (Hakami and Barton, 1990). According to Hakami and Barton's works, the apertures between two walls of fracture are distributed by a log-normal or Gaussian law. This type of apertures has been used in most of numerical and analytical studies of the fluid flow and the solute transport in single fractures with variable apertures (Pyrak-Nolte et al., 1988; Renshaw, 1995).

The laboratory experiments showed that the apertures in a fracture are spatially correlated (Pyrak et al., 1987). Moreno et al. (1988), Tsang and Tsang (1987), and Ewing and Jaynes (1995) introduced a geostatistical method to describe the spatial correlation of variable apertures generated by the law of lognormal distribution. Brown (1989), Thompson and Brown (1991), and Oron and Berkowitz (1998) utilized the method of fractal geometry. This method is based on the fact that the topographical profiles of natural fracture surfaces decrease in the power of the spectral density function with the same form as those of fractal surfaces.

In this study, we assume that variable apertures in a single fracture are generated by the law of normal distribution and the fracture surface roughness is represented by using a self-affine fractal model. The self-affine fractal surface is characterized by its fractal dimension D and looks 'similar to itself' when the length scales in the x- and y-direction are rescaled by factors a and b, and the length scale in the z-direction is rescaled simultaneously by the factor b'. Fig. 1 illustrates an example of fractal surface generated on a lattice of size 64×64 by using two different values of D. It can be shown that the fractal surface with $D = 2.0$ is smoother than that with $D = 2.5$.

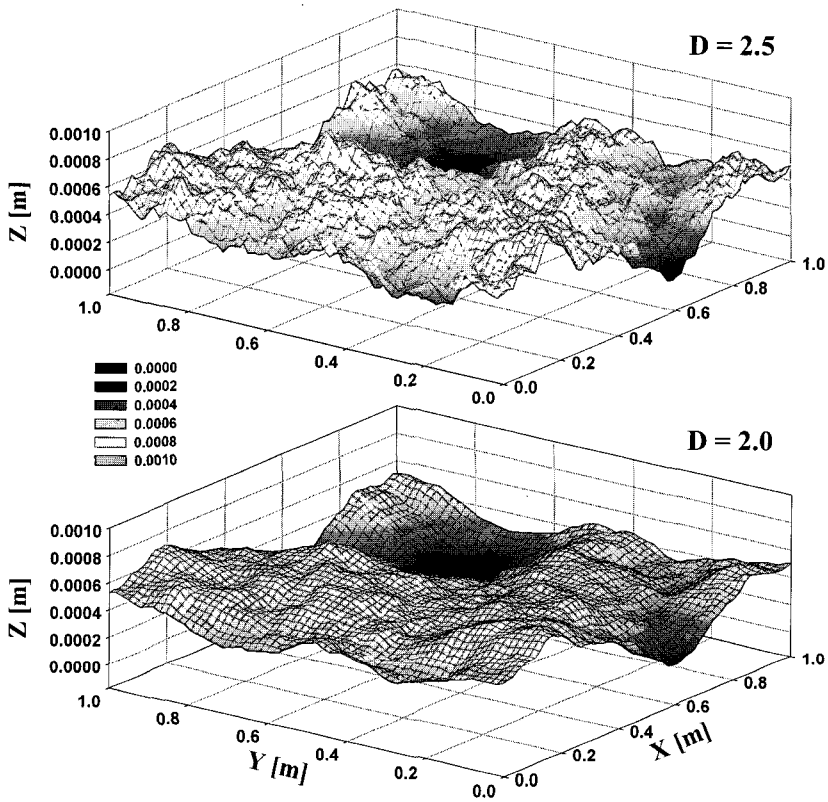

Fig. 1 Fractal surface generated using a Fourier filtering algorithm on a lattice of size 64 × 64. (a) D = 2.0, (b) D = 2.5.

3. LOCAL FLUID FLOW MODEL AT SINGLE FRACTURE SCALE

Once the variable apertures are generated in a single fracture which is discretized into square grids, each cell of size a being characterized by its own aperture e, the local flow can be calculated by taking the following hypotheses: 1) the fluid flow takes place in the laminar range, 2) the cubic law is locally valid at the fracture cell's scale. The hydraulic conductivity between cells i and j is calculated as harmonic mean. The volumetric flow rate Q between cells i and j with apertures e_i and e_j, respectively, is then proportional to the hydraulic head gradient, as follows:

$$Q_{ij} = \frac{g}{12\nu} \frac{2\Delta a}{\left(\frac{1}{e_i^3} + \frac{1}{e_j^3}\right)} \left(\frac{h_i - h_j}{\Delta a}\right) \tag{1}$$

where g [ms^{-2}] denotes gravitational acceleration, ν [m^{2}s^{-1}] is kinematic viscosity and h_i and h_i are hydraulic heads at cells i and j, respectively.

In a steady-state flow condition, the principle of mass conservation at node i connecting to j other nodes can be written as the following equation:

$$\sum_j Q_{ij} = 0 \tag{2}$$

After prescribed unit hydraulic heads (1 m/m) at two opposite boundaries (Fig. 2), Equation (2) can be solved for the global flow in a single fracture. No flow condition is imposed at two boundaries parallel to the flow direction.

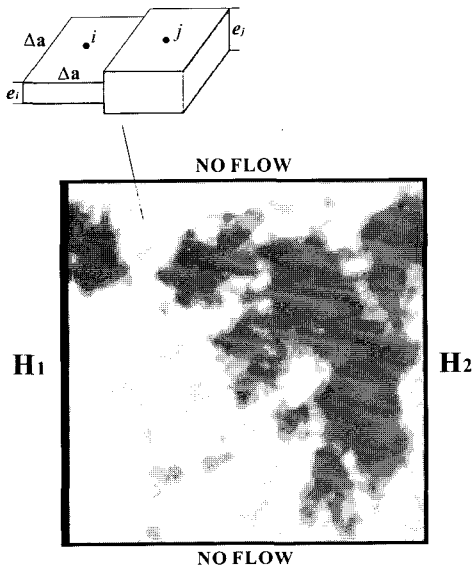

Fig. 2 Schematic illustration of fluid flow through a single fracture with variable apertures. H_1 and H_2 are the global hydraulic heads prescribed at two opposite boundaries ($H_1 > H_2$).

A five-point finite difference scheme using an iterative preconditioning conjugate gradient method is adopted to solve a system of linear equations from Equation (2). The solution of this system yields the hydraulic head at each node, except for the nodes at the left and right boundaries. The volumetric flow rate between adjacent nodes is then calculated using Equation (1).

4. HYDROMECHANICAL COUPLING AT SINGLE FRACTURE SCALE

In order to consider the effect of normal stresses on the flow and transport in the fracture, a nonlinear relationship between the normal stress and closure displacement (or mechanical aperture) was combined with the local flow model. It was assumed that this relationship is valid at the scale of the fracture itself. An empirical hyperbolic formula (Bandis et al., 1983) is used for the simulation

$$\sigma_n' = \frac{k_{n0}\,\Delta u\, e_0}{e_0 + \Delta u} \tag{3}$$

where σ_n' [MPa] is the effective normal stress, k_{n0} [MPa · L^{-1}] is the initial normal stiffness coefficient at zero effective normal stress, e_0 [L] is the maximum closure (i.e. the initial mean aperture at zero normal stress) and u [L] is the closure displacement under a specified effective normal stress.

Given an initial normal stiffness coefficient and a maximum closure value for a fracture, the available aperture for the flow at a specified effective normal stress is derived as follows:

$$\Delta u = \frac{\sigma_n e_0}{(e_0 k_{n0} - \sigma_n)} \tag{4a}$$

$$e = e_0 + \Delta u = e_0\left(1 + \frac{\sigma_n}{(e_0 k_{n0} - \sigma_n)}\right) = e_0 F \tag{4b}$$

Substituting Equation (4) into (1), the volumetric flow rate through nodes i and j under a specified normal stress can be calculated from

$$Q_{ij} = \frac{g}{12\nu}\frac{2\Delta a}{\left(\frac{1}{e_{0i}^3 F_i^3} + \frac{1}{e_{0j}^3 F_j^3}\right)}\left(\frac{h_i - h_j}{\Delta a}\right) \tag{5}$$

where e_{0i} and e_{0j} are the maximum closures

(or initial mean aperture at zero normal stress) at nodes i and j, respectively.

The initial normal stiffness coefficient of 25000 MPa·m^{-1} was used in all simulations. After generating the variable aperture distributions at zero normal stress or closure displacement, we reconstruct a new aperture distribution by eliminating elements with apertures smaller than a given closure displacement. In this case, eliminated elements are replaced into contact areas where the flow does not occur.

Each time the closure displacement was uniformly increased, the fractional ratio of contact area, the mean aperture and standard deviation were calculated. The parameters and its values used in this numerical study are listed in Table 1. These values are obtained from various hydraulic tests performed in the geothermic research area of Soult-sous-Forêt in France (Bruel, 1997).

In our numerical simulation, the closure was uniformly increased and the transport behaviors of fluid and solute induced by this compliant effect were investigated.

5. SOLUTE TRANSPORT MODEL AT SINGLE FRACTURE SCALE

Once the steady-state flow is numerically simulated, the transport simulation through the single fracture will be carried out using the particle following algorithm. Particles were randomly introduced along the upstream boundary. When particles arrive at intersection, they reorient toward one of out-going branches with a sampling and a probability proportional to the local flow rate (Fig. 3).

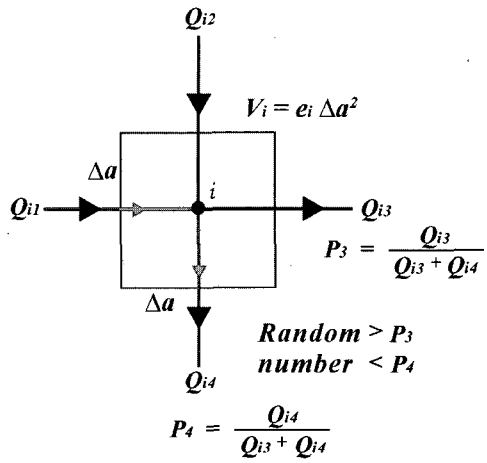

Fig. 3 Choice of particle path at the intersection i. Black line indicates the flow direction and gray line is the particle path. Random number has a range between 0 and 1

Assuming that particles are inert and that no matrix diffusion occurs, the mean residence time t_i of a particle in each square element i is calculated as follows:

$$t_i = \frac{V_i}{\sum_j Q_{ij}} = \frac{e_i \Delta a^2}{\sum_j Q_{ij}} \tag{6}$$

where e_i [m] is an aperture of element i and V_i [m^3] is a volume of element i.

The summation of these mean residence times along channels from the upstream boundary to downstream boundary gives the total residence time of the particle. This calculation was repeated for many particles (for example, 10000) and the result obtained was represented by a breakthrough curve on the downstream boundary.

Table 1. Parameters and its values used in a numerical simulation (Bruel, 1997)

Parameters	Values
Initial mean aperture, e_0 [μ m]	425.0
Standard deviation, m [μ m]	153.0

In this transport simulation, we focus on the dispersion effect of particles resulting from the combination of different pathways in the single fracture with variable apertures. Therefore, we do not consider the effects of molecular diffusion, matrix diffusion or local dispersion within each channel. The global behavior of particle transport for the different realizations can be characterized by the mean residence time and dispersion (Moreno et al., 1988). The mean residence time t_m and its variance S^2_m may be used to determine the Peclet number P_e which is a dimensionless measure of the dispersivity

$$P_e = \frac{t_m^2}{2S_m^2} \tag{7}$$

where

$$t_m = \int \frac{C(\infty) - C(t)}{C(\infty)} dt \tag{8}$$

$$S_m^2 = 2\int_0^\infty t \frac{C(\infty) - C(t)}{C(\infty)} dt - t_m^2 \tag{9}$$

where $C(\infty)$ is the asymptotic tracer concentration which is equal to the initial tracer concentration C_0.

For higher dispersion, S^2_m is considerably influenced by the tail of the breakthrough curve. The Péclet number P_e obtained by using Equation (7) is thus dominated by the tail of the breakthrough curve. An alternative method calculating P_e is to use the dispersion estimator from the arrival times for $C(t)/C_0$=0.1, 0.5 and 0.9 and is used in our study. From a breakthrough curve, the dispersion estimator is calculated (left in Fig. 4) and the Péclet number is determined from a curve of P_e versus dispersion estimator (right in Fig. 4). This curve is obtained from the solution of the advection-dispersion equation for a porous medium (Neretnieks et al., 1982). In most case, the Péclet number calculated using this method is larger than that calculated from Equation (5) (Moreno et al., 1988).

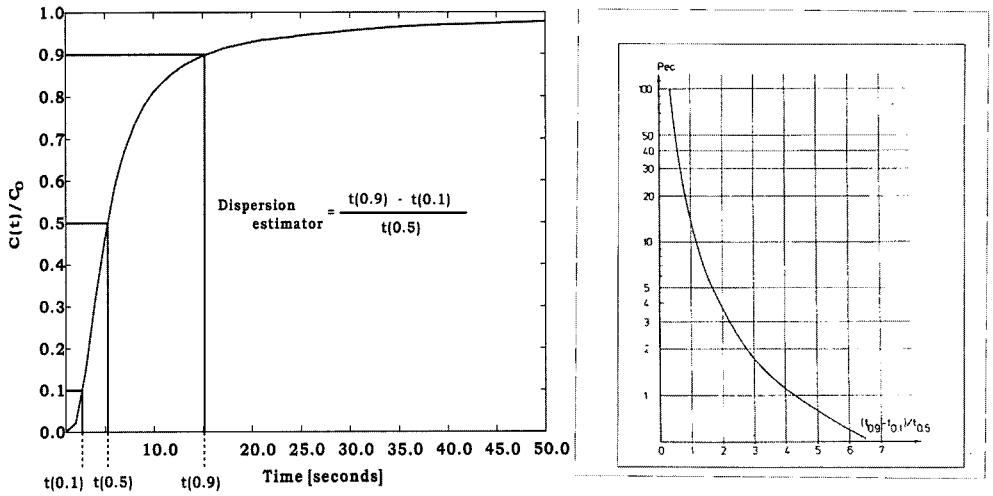

Fig. 4 Calculation of the dispersion estimator (right) and the curve representing the relationship between P_e and dispersion estimator (Neretnieks et al., 1982).

6. NUMERICAL RESULTS

6.1 Flow Simulations

Flow simulations were carried out in 10 independent aperture distributions at each level of the effective normal stress and all of results correspond to mean values for 10 realizations. As an example, Fig. 5 illustrates the distributions of local flow rate for D = 2.5 and 2.2 at σ_n' = 11.95MPa. One can observe that the flow paths in D = 2.5 is more tortuous than those in D = 2.0.

Fig. 6 shows variations of the effective permeability of fracture with the effective normal stress for D = 2.5 and 2.2. In both cases of D, the effective permeability decreases non linearly, but the fracture of D = 2.2 is slightly more permeable than that of D = 2.5. This result is the same as that by several researchers such as Moreno et al.(1988), Ewing and Jaynes(1995).

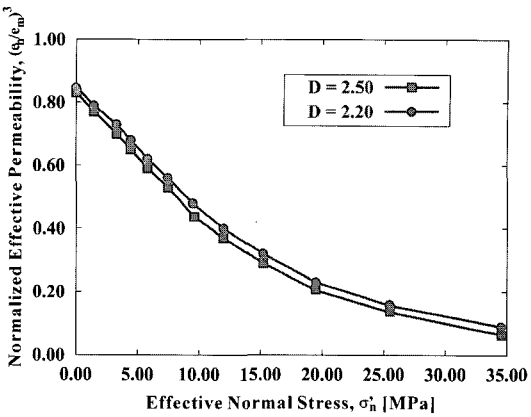

Fig. 6. Variations of the effective permeability of fracture with the effective normal stress for D = 2.5 and 2.2

The relationships between the ratio of mean effective aperture (e_m) and its standard deviation (σ_m) and the third power of normalized effective

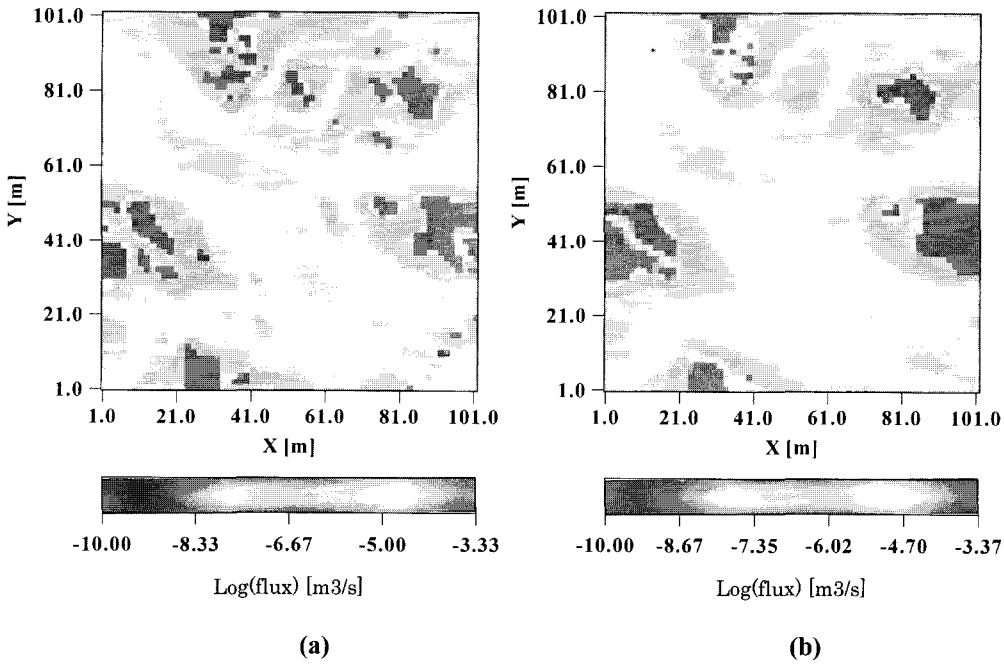

Fig. 5 Distributions of local flow rate at σ_n'=11.95 MPa for two different values of D=2.5 (a) and 2.2 (b)

permeability $(e_h/e_m)^3$ of fracture are shown in Fig. 6 for D= 2.5 and 2.2. This ratio represents the mean separation between two walls in a rough fracture and can be considered as a measure of fracture roughness, and e_m and e_h are the mean aperture and the hydraulic aperture calculated from the cubic law at each level of σ_n', respectively .

When the ratio decreases, the effective permeability decreases showing almost identical tendency between D = 2.5 and 2.2. This tendency of effective permeability is similar to that obtained from Thomson's work (1991). We also compared with results obtained from Zimmerman and Bodvarsson's analytical model (1996), which is expressed by:

$$\left(\frac{e_h}{e_m}\right)^3 = \left[1-1.5\left(\frac{\sigma_m}{e_m}\right)^2\right](1-2c) \qquad (10)$$

where c is a ratio of zones in contact.

As a result of the comparison, a relatively good agreement between the numerical model and Zimmerman and Bodvarsson's model is obtained for both D= 2.5 and 2.2 (Fig. 7).

6.2 Transport Simulations

Fig. 8(a) shows the variation of mean transit time of particles with the effective normal stress for D= 2.5 and 2.2. The mean transit time in both cases of D increases non-linearly with the effective normal stress and the case of D= 2.5 increases faster than that of D= 2.2. However, the difference between two values of D is gradually increased with the effective normal stress. This result is due to the fact that the particle pathway in the fracture with D= 2.5 is more tortuous flow path than that in the fracture with D= 2.2 (Fig. 8(b)). Consequently, the solute transport in a single fracture is influenced by the effective normal stress as well as the fracture surface roughness.

In a rough fracture, there are always continuous flow paths composed of relatively large apertures. These flowpaths are referred to as "*critical flow paths*" along which most of flow takes place (David, 1993). The analysis of critical flow paths was used as a tool for identifying the

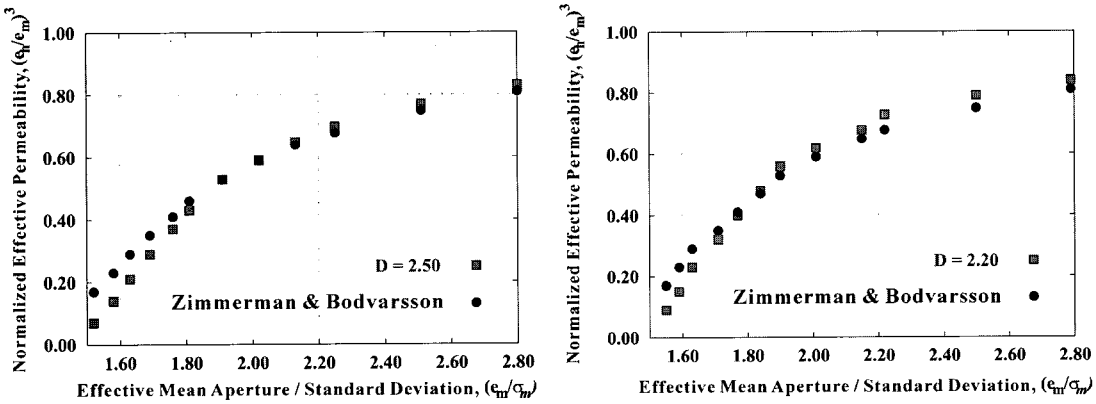

Fig. 7 Relationship between the effective permeability and the normalized effective permeability $(e_h/e_m)^3$ for D= 2.5 (a) and 2.2 (b), and the comparison with Zimmerman and Bodvarsson's model.

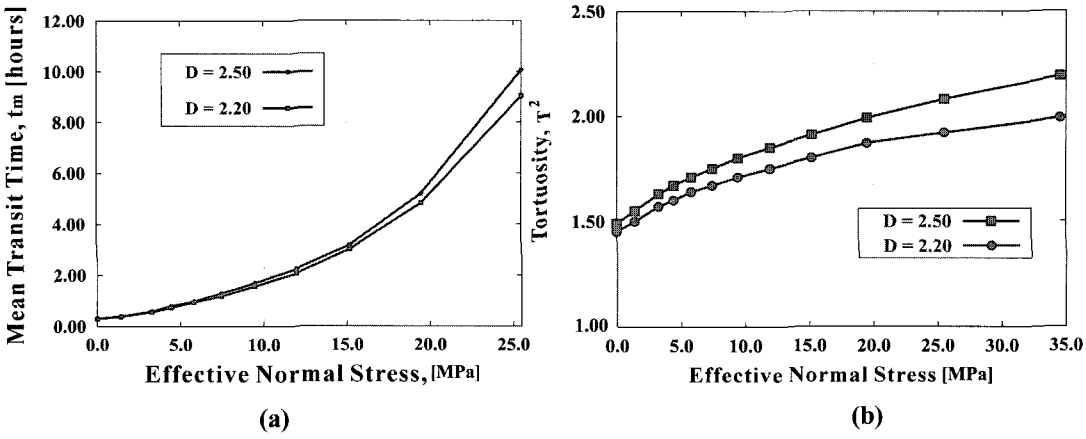

Fig. 8 Variations of mean transit time (a) and tortuosity (b) with the effective normal stress. $T^2 = (L_{real} / L)^2$, where L_{real} is the real distance transported by the particles, and L is the distance of the straight streamline parallel to the flow direction

conduction process in a heterogeneous medium and is to find the optimal path which carries the significant portion of the total flow rate in the flow network.

David (1993) proposed a method to characterize quantitatively the geometry of flow paths in the two-dimensional heterogeneous network. This method is to seek elements which carry more than a given portion X of the total flow rate, diminishing the value of X step by step until one continuous path appears in the network. David (1993) defined such a continuous path as the "*most efficient path*" for the flow and observed from his numerical studies that this path does not remain the same for the different levels of the effective normal stress.

In the present study, we suggested another method in which the most efficient path is determined by identifying each particle's trajectory that is a continuous line between the upper and lower boundaries. For each trajectory, the local flow rate varies from one element to the other and thus the process is to seek the element with the highest local flow rate for each particle. By this process, we obtain one continuous path which represents the best solution for carrying the largest amount of flow. Fig. 9 shows the most efficient path for three different values of σ_n' in both D = 2.5 and 2.2. It can be seen that these paths are different as a function of σ_n'. This result is consistent with that obtained by David (1993).

The ratio of the flow rate through the most efficient path Q_{mep} to the global flow rate Q_{eff} is presented in Fig. 10 as function of σ_n'. For both case of D = 2.5 and 2.2, the ratio Q_{mep} / Q_{eff} increases as σ'_n increases. This means that the role of the most efficient path for the flow becomes important gradually as the connectivity between elements is reduced. We can also observe that the ratio Q_{mep} / Q_{eff} in the case of D = 2.5 is generally higher than that in the case of D = 2.2, according to increasing σ_n'.

Fig. 11 shows the variation of the Péclet number with the effective normal stress. This number is a dimensionless measure of the dispersivity and is calculated by the same method as that performed by Moreno et al. (1988). We can see that there is no apparent difference

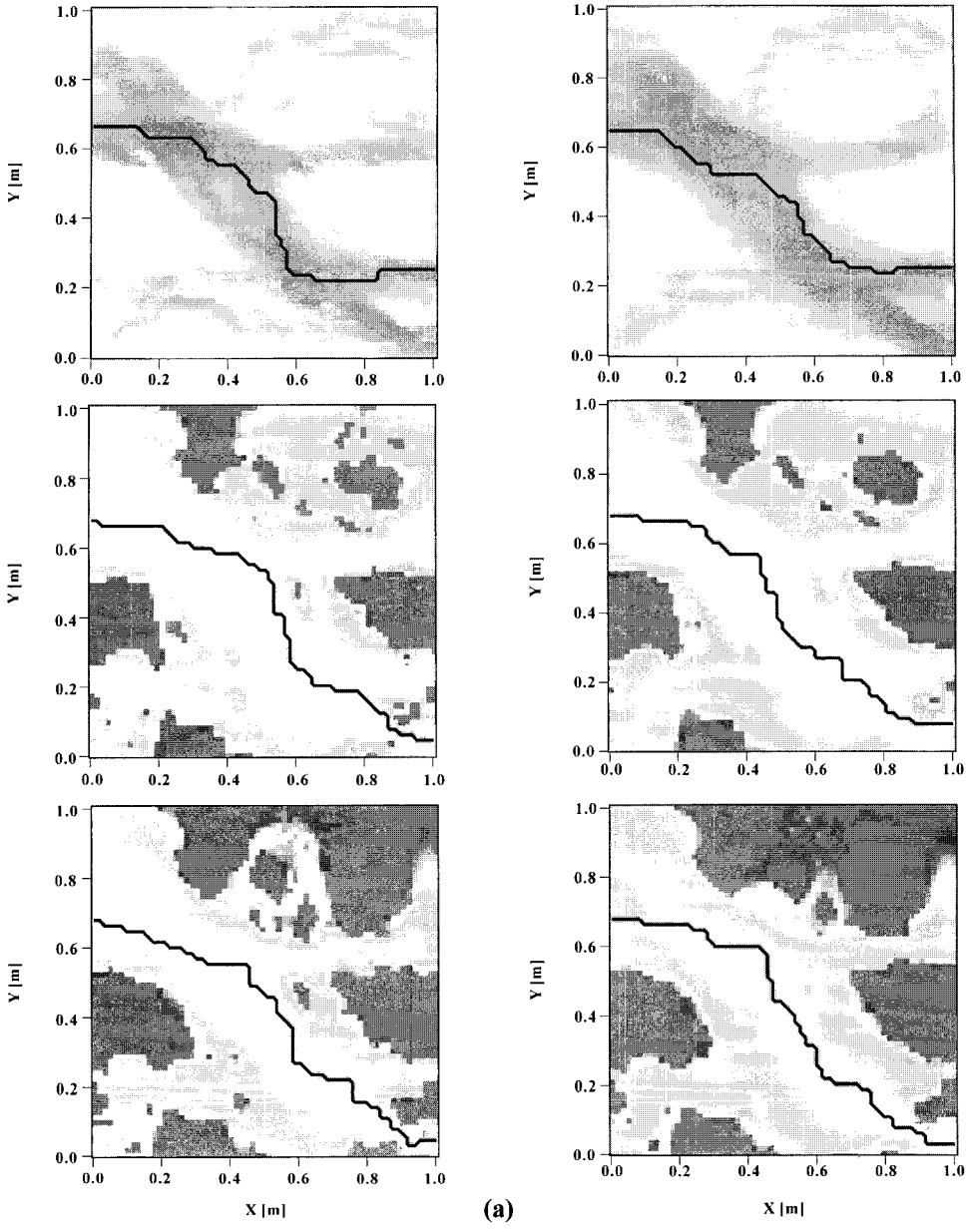

Fig. 9 Most efficient paths for the three different values of the effective normal stress in both D= 2.5(a) and 2.2(b): from top 0.0, 25.0 and 30.0 MPa. The solid lines represent the most efficient paths

between D= 2.5 and 2.2. The number of Péclet decreases very rapidly up to 5.8MPa of σ_n'. This result means that the channels provided to particles are progressively reduced by zones in contact increasing as σ_n' increases. After this threshold, most of particles displace only along one or two main channels.

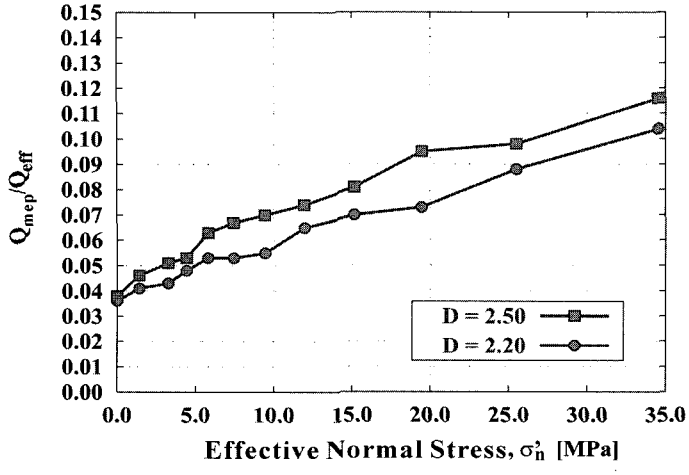

Fig. 10 Relationship between the ratio Q_{mep}/Q_{eff} and the effective normal stress for both D = 2.5 and 2.2

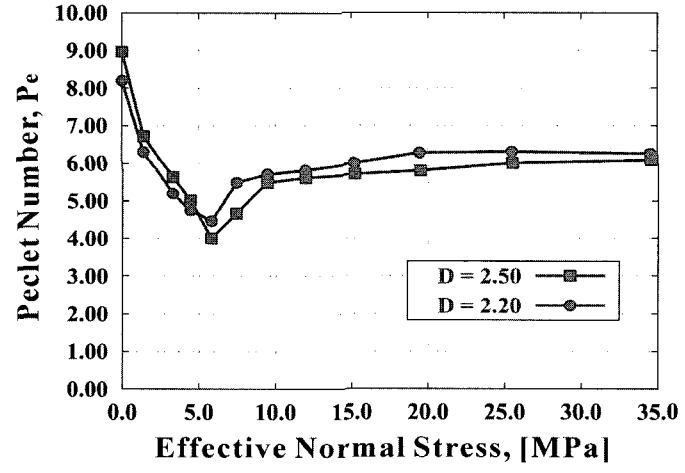

Fig. 11 Variations of number of Péclet with the effective normal stress for D= 2.5 and 2.2.

7. CONCLUSION

We studied numerically the hydromechanical behaviors of the fluid flow and solute transport in a single rough fracture generated by the self-affine fractal model. It can be observed that the effective permeability of this fracture depends strongly on the aperture distribution varying with the effective normal stress but does not on the fracture roughness. The results obtained from the flow simulations are a good agreement with those predicted by Zimmerman and Bodvarsson's empirical model.

The characteristics of the fluid flow in a fracture are significantly influenced by the effective normal stress but slightly by the fracture surface roughness. However, we observed that the solute transport in a fracture is strongly affected by the effective normal stress as well as the fracture surface roughness. According to the variation of the Péclet number with the effective

normal stress, once the effective normal stress arrives at certain level (i.e. 11.95 MPa in our study), these channels have almost the same form. Moreover, the particles displace only along the channel reduced and thus the spatial dispersion of particles becomes constant.

We can expect that the results obtained from these numerical studies will be helpful to describe the characteristics of flow and transport with the hydromechanical effect for each element consisting of the three-dimensional fracture network.

REFERENCES

Bandis, S. C., A. C. Lumsden and N. R. Barton (1983), "Fundamentals of rock joint deformation", *International Journal of Rock Mechanics and Mining Sciences.*, Vol. 20, No. 6, pp. 249-268.

Brown, S. R. (1989), " Simple mathematical model of a rough fracture" , *Journal of Geophysical Research*, Vol. 100, No. B4, pp. 5941-5952, 1987.

Bruel, D. (1997), "Solute transport in a discrete fracture network model with nonlinear hydromechanical interactions", European HDR geothermal project, JOR3-CT95-0054, Rapport C.I.G, Ecole des Mines de Paris, LHM/RD/97.

Durham, W.B. and Bonner, B.P. (1995), "Closure and fluid flow in discrete fractures", In Fractured and Jointed Rock Masses, (eds). L.R. Myer, N.G.W. Cook, R.E. Goodman and C.-F. Tsang, Balkema, Rotterdam, pp. 441-446.

Ewing, P. R. and D. B. Jaynes (1995), "Issues in single-fracture transport modeling: Scales, algorithms, and grid types", *Water Resources Research*, Vol. 31, No. 2, pp. 303-312.

Gentier, S. (1986), "Morphologie et comportement hydromécanique d'une fracture naturelle dans un granite sous contrainte normale : étude expéimentale et théorique", Ph. D. Dissertation, Université d'Orléns, France.

Hakami, E. and N. Barton (1990), "Aperture measurements and flow experiments using transparent replicas", In Barton N. and O. Stephansson (eds.), Rock Joints, Proc. Intern. Symp., Leon, Norway, 4-6 June, Rotterdam, Balkema.

Moreno, L., C. F. Tsang, Y. Tsang, F. V. Hale and I. Neretnieks (1988), "Flow and tracer transport in a single fracture: A stochastic model and its relation to some field observations", *Water Resources Research*, Vol. 24, No. 12, pp. 2033-2048.

Oron, A. P. and B. Berkowitz (1998), "Flow in rock fractures: The local law assumption reexamined", *Water Resources Research*, Vol. 34, No. 11, pp. 2811-2825.

Pyrak-Nolte, L. J., N. G. W. Cook and D. D. Nolte (1988), "Fluid percolation through single fractures", *Geophysics Research Letters*, Vol. 15, No. 11, pp. 1247-1250.

Renshaw, C. E. (1995), "On the relationship between mechanical and hydraulic apertures in rough- walled fractures", *Journal of Geophysical Research*, Vol. 100, No. B2, pp. 24629-24636.

Thompson, M. E. (1991), "Numerical simulation of solute transport in rough fractures", *Journal of Geophysical research*, Vol. 96, No. B3, pp. 4157-4166.

Thompson, M. E. and S. R. Brown (1991), "The effect of anisotropic surface roughness on flow and transport in fractures", *Journal of Geophysical Research*, Vol. 96, No. B13, pp. 21923-21932.

Tsang, Y. W. and C. F. Tsang (1987), "Channel model of flow through fractured media", *Water Resources Research*, Vol. 23, No. 3, pp. 467-

479.

Yeo I.W., de Freitas, M.H. and Zimmerman, R.W. (1998), "Effect of shear displacement on the aperture and permeability of a rock fracture", *International Journal of Rock Mechanics and Mining Sciences*, Vol. 35, No. 8, (1998), pp. 1051-1070.

Zimmerman, R. W. and G. S. Bodvarsson (1996), "Hydraulic conductivity of rock fractures", *Transport in Porous Media*, No. 23, pp. 1-30.

Hydrosystems Engineering Center, Korea Institute of Water and Environment, Korea Water Resources Corporation, 462-1 Jeonmin-Dong, Yusung-Gu, Daejeon, 305-730, Korea

(E-mail: jeongwc@kowaco.or.kr)

Hydrosystems Engineering Center, Korea Institute of Water and Environment, Korea Water Resources Corporation, 462-1 Jeonmin-Dong, Yusung-Gu, Daejeon, 305-730, Korea

(E-mail: mhhwang@kowaco.or.kr)

Hydrosystems Engineering Center, Korea Institute of Water and Environment, Korea Water Resources Corporation, 462-1 Jeonmin-Dong, Yusung-Gu, Daejeon, 305-730, Korea

(E-mail: ihko@kowaco.or.kr)

Department of Civil Engineering, Hongik University, 72-1, Sangsu-Dong, Mapo-Gu, Seoul, 121-791, Korea

(E-mail: jwsong@hongik.ac.kr)